J. Fluid Mech. (1987), *vol.* 174, *pp.* 467–493
Printed in Great Britain

Multiple solutions and flow limitation for steady flow through a collapsible tube held open at the ends

By J. W. REYN

Subdepartment of Mathematics and Informatics, Delft University of Technology, Julianalaan 132, 2628 BL Delft, The Netherlands

(Received 14 December 1984 and in revised form 29 May 1986)

Equations for the steady flow of an incompressible, inviscid fluid through a collapsible tube under longitudinal tension are derived by treating the tube longitudinally as a membrane, and taking the collapsibility of the tube into account in an approximate way by replacing in the equation for an axisymmetric membrane a term representing the resistance of the tube to area change by the tube law for collapsible tubes. The flow is assumed to be uniform in a cross-section. A nonlinear differential equation is obtained for the shape of the tube for given values of total pressure p_0, flow rate q, longitudinal tension τ and tube law $P = P(\rho)$; where $\rho = (A/\pi R^2)^{\frac{1}{2}}$ is the equivalent radius of the tube (A = area of a cross-section, R = radius of the unloaded, then circular tube). The equation can be integrated and analysed in the phase plane. Equilibrium points correspond to uniform flow through cylindrical tubes; saddle points correspond to subcritical flow ($S < 1$), centrepoints to supercritical ($S > 1$) and a higher-order point to critical flow ($S = 1$). Here S is the speed index, the ratio of the flow speed to the speed of long waves. Near centrepoints there are solutions, that represent area-periodic tubes. For a finite tube, held open at the ends, the steady flow is formulated as a two-point boundary-value problem. On the basis of numerical calculations, and a bifurcation analysis using the method of Lyapunov–Schmidt, the existence and multiplicity of the solutions of this problem are discussed and the process of flow limitation studied. For negative total pressures two collapsed solutions are found that disappear at the flow-limitation value of the flow rate. For positive total pressures a distinction is made between subcritical, critical and supercritical total pressures. In all these cases there is a multiplicity, proportional to the ratio of the tube length to $\mathscr{L}_1(0)$, the wavelength of the collapsed periodic solution for vanishing flow rate, and having maximum radius $\rho = 1$. For subcritical total pressures increase of the flow rate leads to a gradual loss of all solutions in higher-order flow limitations until final flow limitation occurs by the mergence of two collapsed solutions. For supercritical total pressures increase of the flow rate also leads to a gradual loss of all solutions in higher-order flow limitations in a process which now also depends upon the ratio of the tube length to the wavelength L of periodic solutions with vanishing amplitude and $\rho \equiv 1$.

1. Introduction

A collapsible tube is an elastic tube characterized by the fact that it changes drastically in cross-sectional shape (and area) owing to small changes in transmural pressure (the difference between the internal and external pressure) close to zero.

Flows through such tubes are of physiological interest in relation to flow of blood through veins (and to some extent through arteries), air flow through the pulmonary airways and flow through the urinary tracts, to list a few examples (Shapiro 1977; Pedley 1980). Also, technical applications are known, such as the flexible cold-water pipe used in ocean-thermo-energy installations to bring the cold water in deep oceans up and in contact with the warmer surface water in order to derive energy. There have been a large number of laboratory experiments to investigate the properties of collapsing tubes with segments of rubber tube, often spanned between rigid inlet and outlet tubes and contained in a pressurized chamber. Incompressible fluid flows along the tube from a constant-head reservoir, and the flow rate can be controlled by adjusting the resistances of the rigid parts of the system upstream and downstream of the collapsible segment. In these experiments 'flow limitation' can be observed, showing the phenomenon that the flow rate cannot continue to be increased by lowering the pressure just downstream of the collapsible segment further, while keeping the pressure upstream of the segment and that in the pressurized chamber constant. A common result in these experiments has also been the appearance of self-excited and self-sustaining oscillations in the tube cross-sectional area and the outflow velocity for a range of values of the governing parameters (Conrad 1969; Katz, Chen & Moreno 1969; Ur & Gordon 1970; Brower & Scholten 1975; Griffiths 1977; Bonis & Ribreau 1978; Lyon *et al.* 1981; Bertram 1982).

Several models have been proposed both for the excitation and for the perpetuation of these oscillations, incorporating various physical mechanisms that seem to be important. One such mechanism is 'choking' (Shapiro 1977, p. 135), which occurs when at any point along the collapsible tube the cross-sectionally averaged fluid velocity in the tube attains the local value of the speed of propagation of small-amplitude pressure waves, whereas at the same time a steady-flow solution becomes impossible in a one-dimensional model in which the elastic properties of the tube are represented by a 'tube law', i.e. the transmural pressure at any point is taken to be a single-valued function of the cross-sectional area at that point. Breakdown of steady flow through choking seems to have occurred in several experiments, as reported for example by Brower & Scholten (1975), Griffiths (1977) and Bonis & Ribreau (1978). It is usually connected with 'flow limitation', since in a dynamic explanation of this phenomenon a lowering of the downstream pressure sends an expansion wave upstream which cannot pass the point where the flow is 'critical' (flow speed equals wave speed). Roll-wave instability has also been suggested, which is associated with the variation of viscous resistance with cross-sectional area (Pedley 1980). A mechanism that can trigger off oscillations in 'subcritical' (flow speed less than wave speed) flow also, although it causes much stronger oscillations in 'supercritical' flow, has been modelled by Pedley (1980), Bertram & Pedley (1982) and Cancelli & Pedley (1985). A critical factor in this mechanism is the amount of energy lost in the flow emerging as a turbulent jet from the time-dependent constriction in the collapsible tube. The dynamics of the oscillations is then dominated by longitudinal movement of the point of flow separation, in response to the adverse pressure gradient associated with waves propagating backwards and forwards along the collapsible tube. A model incorporating this mechanism should include the important constraints exerted on such oscillations by the mechanical properties of the upstream and downstream rigid segments (Cancelli & Pedley 1985). One feature that is known to be important in many experiments, i.e. longitudinal tension in the tube wall which provides a force resisting collapse in addition to the force provided by the transverse bending stiffness of the tube wall, has only recently been included in the modelling of this mechanism

(Cancelli & Pedley 1985). The effects of longitudinal tension were taken into account by a correction term added to the tube law in a manner similar to that of McClurken *et al.* (1981), who studied theoretically steady, supercritical flow in collapsible tubes with a shock-like transition to subcritical flow, in addition to the experimental study by Kececioglu *et al.* (1981) on the same subject. The motion of fluid and wall was studied by solving numerically an initial-boundary-value problem for a fourth-order system of differential equations involving x and t as independent variables, where x is measured along the tube axis and t is time. The boundary conditions correspond to a collapsible tube held open at its ends and to the pressures there dictated by the mechanical properties of the rigid parts of the system and the pressures far upstream and far downstream. The initial state was taken to be one in which the collapsed segment has uniform area and the velocity is uniform and subcritical. Collapse of the tube is then initiated by increasing the pressure in the surrounding chamber over a short time to a higher constant value. In some cases a steady state is eventually set up and in some cases oscillations develop.

The study presented in the present paper was motivated by the wish to obtain a better understanding of possible mechanisms of self-excited oscillations in collapsible tubes when the effects of longitudinal tension are taken into account. Apart from the mechanism modelled by Cancelli & Pedley (1985) in which flow separation plays an essential role, oscillations are also predicted by a highly simplified model of the hydraulic circuit as a mass-spring system, and also when neglecting dissipation effects altogether (Schoendorfer & Shapiro 1977). Before studying a possible inviscid mechanism for these unsteady flows, it is of interest to study the question of the existence and stability of steady inviscid flow of an incompressible fluid through a collapsible tube held open at the ends, thereby excerting a longitudinal pulling force on the tube. In this paper the emphasis will be on the first question by deriving a nonlinear differential equation for the shape of the tube, i.e. the change of cross-sectional area with distance along the tube and by formulating a two-point boundary-value problem to find the shape of a tube held open at the ends. On the basis of numerical calculations for various sets of values of total pressure p_0, flow rate q, a given pulling force τ, and the results of a bifurcation analysis for some specific values of these parameters, the existence and multiplicity of solutions will be discussed. In particular what happens when, for a given value of the total pressure, the flow rate is given increasing values will be discussed, thus also describing the process of 'flow limitation'. Although inviscid flow is the object of this paper, and further research is needed to access viscous effects on the results, if separation occurs, the present calculations also provide a basis for comparison with experimental results. The main point to be made now, however, is to emphasize qualitative effects such as the multiplicity of solutions of the boundary-value problem and the process of flow limitation.

2. Steady flow of an inviscid, incompressible fluid through a cylindrical collapsible tube. Flow limitation in cylindrical tubes

The steady flow of an inviscid, incompressible fluid through a cylindrical (not necessarily circular) collapsible tube is a relatively easy case to study and the effects of longitudinal tension are not difficult to access. In the rest of the paper we shall need these flows, however, as special solutions. Moreover, some idea of how a multiplicity of solutions of the boundary-value problem arises and how the process of 'flow limitation' develops may be obtained from simple considerations. Let A be

the cross-sectional area of the tube, ρ_f the density of the inviscid, incompressible fluid which is flowing with a uniform speed V and let P_0 be the total pressure in the flow. Then, Bernoulli's equation may be written as

$$P = P_0 - \tfrac{1}{2}\rho_f V^2 = P_0 - \frac{\rho_f Q^2}{2A^2}, \tag{1}$$

where P is the pressure in the tube, and $Q = VA$ is the (constant) volume flow through the tube. Let pressures be measured as differences with the pressure outside the tube, which is assumed to be constant. Since we want to consider elastic tubes, we non-dimensionalize (1) using R, t and E, being the inner radius of the then circular tube at zero pressure, the thickness of the undeformed wall and Young's modulus of the elastic material respectively. Then, with

$$\rho = \left(\frac{A}{\pi R^2}\right)^{\frac{1}{2}}, \quad p = \frac{PR}{Et}, \quad p_0 = \frac{P_0 R}{Et}, \quad q = \frac{Q}{\pi}\left(\frac{\rho_f}{2EtR^3}\right)^{\frac{1}{2}}, \tag{2}$$

(1) may be written as

$$p = p_0 - \frac{q^2}{\rho^4}. \tag{3}$$

Because of the elasticity of the tube, its cross-sectional area changes with pressure; for collapsible tubes the relation between the two is called the 'tube law'. In the literature several discussions may be found with regard to proper forms of this 'tube law' (Shapiro 1977; Pedley 1980; Kececioglu *et al.* 1981; Cancelli & Pedley 1985). If the tube is highly collapsed, such that opposite walls are in contact, stretchless bending theory gives a similarity solution, which is in good agreement with experimental observations (Kececioglu *et al.* 1981). Then

$$\frac{PR}{Et} = P(\rho) = -\frac{\beta}{\rho^3}, \tag{4}$$

where $\beta = \frac{1}{12}t^2/R^2(1-\mu^2)$, and μ is Poisson's ratio. In order to arrive at a simple analytic expression that is consistent with (4) for small ρ and satisfies $P(1) = 0$, a modified similarity law was proposed by Shapiro (1977):

$$P(\rho) = \beta\left(1 - \frac{1}{\rho^3}\right). \tag{5}$$

This law was used in the numerical calculations for $\rho \leqslant 1$, as reported in this paper. For β the value 0.001 was selected, which with $\mu = 0.5$ corresponds to a wall thickness/tube radius ratio of about 0.1. For $\rho \geqslant 1$ a tube law may be derived from membrane theory for a circularly cylindrical tube made of an elastic material obeying Hooke's law

$$P(\rho) = \left(1 - \frac{1}{\rho}\right)\{1 + \mu(1-\rho)\}. \tag{6}$$

It is well known that for an incompressible material $\mu = 0.5$. However, the large stiffening effect when the collapsed tube is pressurized and brought into an inflated (circular) shape occurs even for small values of $\rho - 1$ and, unless quantitative precision is aimed at, for simplicity the term $\mu(1-\rho)$ can be dropped, which effectively can be done by taking $\mu = 0$. Moreover, the use of (6) for large inflations would in any case not be accurate since for large deformations the application of Hooke's law would not be justified. As a result, in the numerical calculations that are reported in the present paper (6) was used with $\mu = 0$, thus accounting for the effect of the larger stiffness of the inflated tube without claiming quantitative precision for larger deformations.

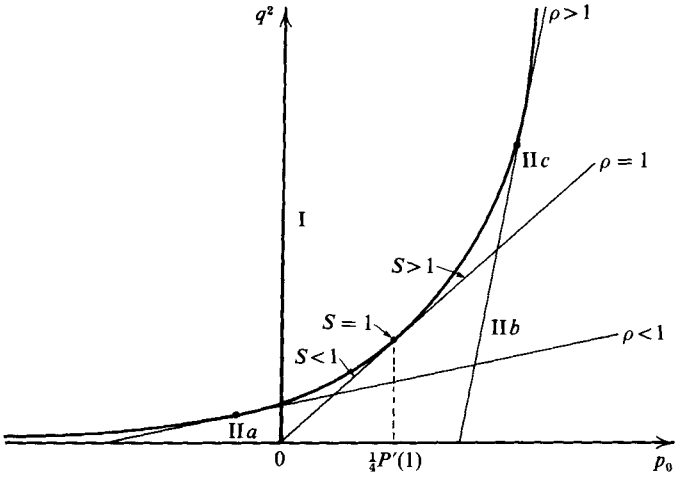

FIGURE 1. Representation of uniform-flow solutions in the parameter plane p_0, q^2; p_0 = total pressure, q = flow rate.

If the tube law is combined with Bernoulli's equation (3), we get

$$p_0\rho^4 - \rho^4 P(\rho) - q^2 = 0, \tag{7}$$

the solutions of which yield the values of the area of a cylindrical collapsible tube that allow the passage of a uniform flow with given total pressure and flow rate. In the (p_0, q^2)-plane, (7) can be represented by a bundle of straight lines on which ρ (and then p) is constant, such as illustrated in figure 1. Only $q^2 > 0$ and values of p_0 between some negative and positive bounds are of interest. For a wide class of tube laws this bundle may be expected to have an envelope separating regions in the (p_0, q^2)-plane with no solutions and more solutions of (7). This may be seen by noting that if for $\rho \to 0$ the tube law satisfies (4), then the line for $\rho = 0$ coincides with $q^2 = 0$, whereas for $\rho = 1$, with $P(1) = 0$ the straight line is given by $q^2 = p_0$, and there is a continuous change with ρ of the slope of the lines ρ = constant. An envelope of (7) is given by

$$p_0 = P(\rho) + \tfrac{1}{4}\rho P'(\rho), \quad q^2 = \tfrac{1}{4}\rho^5 P'(\rho), \tag{8}$$

which thus has the slope $\mathrm{d}q^2/\mathrm{d}p_0 = \rho^4$. Since for $\rho = 0$ the straight line coincides with $q^2 = 0$ and the slope of the envelope vanishes, the envelope approaches the axis $q^2 = 0$ asymptotically as $\rho \to 0$. It has the slope 1 for $\rho = 1$ and the line $\rho = 1$ is tangent to it at $(\frac{1}{4}P'(1), \frac{1}{4}P'(1))$. If we require that the envelope is concave upwards and is represented by a univalent function of p_0, then there exists a region I above the envelope with no solutions of (7) and a region II below the envelope with just two solutions of (7). If on the envelope we require ρ to be an increasing function of p_0, $\mathrm{d}q^2/\mathrm{d}p_0 = \rho^4$ tells us that the envelope is concave upwards. With (8), the condition $\mathrm{d}\rho/\mathrm{d}p_0 > 0$ leads to $\{P(\rho) + \frac{1}{4}\rho P'(\rho)\}' > 0$, which, incidentally, is satisfied for (5) and (6) with $\mu = 0$. In figure 1 the region II is subdivided into three regions: region II*a* with $p_0 < \frac{1}{4}P'(1)$ and above the line $\rho = 1$, containing only collapsed solutions $\rho_1 < \rho_2 < 1$; region II*b* below the line $\rho = 1$ containing a collapsed and an inflated solution $\rho_1 < 1 < \rho_2$; and region II*c* above the line $\rho = 1$ and $p_0 > \frac{1}{4}P'(1)$ containing only inflated solutions $1 < \rho_1 < \rho_2$.

The envelope points at the phenomenon of 'flow limitation', which in this context may be defined as the occurrence of a maximum flow rate that the tube can convey for a given total pressure. When for a given p_0, the flow rate is increased, the two

solutions in region II approach one another and coincide at the maximum flow rate. The solution at flow limitation represents a collapsed tube near region II*a* and an inflated tube near II*c*. In relation to a dynamic explanation of flow limitation it is of interest to relate the flow speed V to the wave speed C of small pressure waves, which may be determined from the tube law given by

$$C = \left(\frac{\mathrm{d}P\{\rho(A)\}}{\mathrm{d}A}\frac{A}{\rho_{\mathrm{f}}}\frac{Et}{R}\right)^{\frac{1}{2}}. \tag{9}$$

The speed index $S = V/C$ will then be

$$S = \frac{2q}{\rho^2(\rho P'(\rho))^{\frac{1}{2}}}. \tag{10}$$

From (8) now follows that on the envelope $S = 1$; so flow limitation occurs when the speeds equals the wave speed. The flow will be called 'critical' in that case, and 'subcritical' for $S < 1$, supercritical' for $S > 1$. The variation of S on a line ρ = constant follows from (8) and (10) and is $S = 0$ for $q^2 = 0$, $S < 1$ on the segment between $q^2 = 0$ and the envelope and $S > 1$ on the segment beyond the point of tangency with the envelope.

3. Steady flow of an inviscid, incompressible fluid through collapsible tubes under longitudinal tension

In a full description as an elastic structure, the collapsible tube is a three-dimensional shell of a complicated shape, experiencing large deformations. At the present stage, however, with grossly simplified models of this structure, valuable information may still be obtained. In particular, some success has been achieved by taking into account longitudinal tension effects in one-dimensional models of flow through collapsible tubes through a correction term added to the tube law (McClurken *et al.* 1981; Cancelli & Pedley 1985). To this end McClurken *et al.* (1981) assumed the tube cross-section to consist of two parallel lines separated by the distance $2y$ and connected by semicircles of radius y. As the separation $2y$ changes, the cross-sectional area also changes. However, if it is assumed that the perimeter is constant and equal to that of a circle of radius $R_0 = \frac{1}{2}D_0 = (A_0/\pi)^{\frac{1}{2}}$ each straight segment is of length $\pi(R_0 - y)$. Thus the cross-sectional area may be expressed as $A = \pi y(D_0 - y)$, and then

$$y = \tfrac{1}{2}D_0\left[1 - \left(1 - \frac{A}{A_0}\right)^{\frac{1}{2}}\right]. \tag{11}$$

The correction term to the tube law is obtained by noting that longitudinal membrane forces in the parallel surfaces of the tube model are capable of supporting a pressure difference, which may be estimated by $\Delta P = -T/R$, where T is the axial force per unit perimeter, assumed to be constant along the tube, and R is the longitudinal radius of curvature in an axial plane. With (11) this leads to

$$\Delta P = -\frac{T}{R} \approx -T\frac{\mathrm{d}^2 y}{\mathrm{d}x^2} = \frac{-T}{\pi D_0}\left[\frac{A_{xx}}{\left(1-\frac{A}{A_0}\right)^{\frac{1}{2}}} + \frac{1}{2A_0}\frac{A_x^2}{\left(1-\frac{A}{A_0}\right)^{\frac{3}{2}}}\right] \approx -\frac{T}{\pi D_0}\frac{A_{xx}}{\left(1-\frac{A}{A_0}\right)^{\frac{1}{2}}}. \tag{12}$$

As stated by McClurken *et al.* (1981), this model becomes quite unrealistic when the tube is nearly round, as also may be expected from the blow up of (12) when $A \to A_0$. In their analysis the factor $(1-(A/A_0))^{\frac{1}{2}}$ in the denominator of (12) is, on occasion, left out on an *ad hoc* basis. Cancelli & Pedley (1985) used another *ad hoc*

assumption by replacing (11) by $y = \frac{1}{2}D_0(A/A_0)$. In the present paper a somewhat different approach is followed, which eventually leads to a result that also may be interpreted as giving a correction to the tube law. The starting point is the observation that inflation to an axially symmetric shape of a thin-walled initially circularly cylindrical elastic tube obeying Hooke's law may quite accurately be described by membrane theory. Let us indicate the tension tangent to the tube surface in the longitudinal direction by σ_1 and in a cross-section by σ_m, and the thickness of the wall under stress by t'; then the equilibrium equations can be

$$\frac{\mathrm{d}}{\mathrm{d}x}\left[\frac{t'\sigma_1 r}{\left[1+\left(\frac{\mathrm{d}r}{\mathrm{d}x}\right)^2\right]^{\frac{1}{2}}}\right] = \tfrac{1}{2}P\frac{\mathrm{d}r^2}{\mathrm{d}x}, \tag{13}$$

for the horizontal equilibrium, and

$$\frac{\mathrm{d}}{\mathrm{d}x}\left[\frac{t'\sigma_1 r\frac{\mathrm{d}r}{\mathrm{d}x}}{\left[1+\left(\frac{\mathrm{d}r}{\mathrm{d}x}\right)^2\right]^{\frac{1}{2}}}\right] + Pr - \sigma_m t'\left[1+\left(\frac{\mathrm{d}r}{\mathrm{d}x}\right)^2\right]^{\frac{1}{2}} = 0, \tag{14}$$

for the vertical equilibrium. Here, $P = P(x)$ is the pressure in the tube and $r = r(x)$ the radius, where x is measured along the tube length. When (13) is substituted into (14), the well-known membrane formula (den Hartog 1952) is obtained:

$$\frac{-t'\sigma_1\frac{\mathrm{d}^2 r}{\mathrm{d}x^2}}{\left[1+\left(\frac{\mathrm{d}x}{\mathrm{d}x}\right)^2\right]^{\frac{3}{2}}} + \frac{t'\sigma_m}{r\left[1+\left(\frac{\mathrm{d}r}{\mathrm{d}x}\right)^2\right]^{\frac{1}{2}}} = P. \tag{15}$$

Furthermore, the following stress–strain relations are valid:

$$\epsilon_1 = \frac{1}{E}(\sigma_1 - \mu\sigma_m), \quad \epsilon_m = \frac{1}{E}(\sigma_m - \mu\sigma_1), \quad \frac{t'}{t} = 1 - \frac{\mu}{E}(\sigma_1 + \sigma_m), \tag{16a, b, c}$$

where ϵ_1 and ϵ_m are the relative strains in the longitudinal and meridional directions respectively. Also we have the geometrical relation

$$\epsilon_m = \frac{r}{R} - 1. \tag{17}$$

For a circular tube, Bernoulli's equation (1) may be written as

$$P = P_0 - \frac{\rho_f Q^2}{2\pi^2 r^4}, \tag{18}$$

which upon insertion in (13) and integration leads to an expression for σ_1:

$$\sigma_1 = \frac{Et}{2t'}\left[\frac{P_0 R}{Et}\frac{r}{R} + \frac{\rho_f Q^2}{2\pi^2 EtR^3}\left(\frac{R^3}{r^3} - \frac{2R}{r}\right) + \lambda\frac{R}{r}\right]\left(1+\frac{\mathrm{d}r}{\mathrm{d}x}\right)^2\Bigg]^{\frac{1}{2}}, \tag{19}$$

where λ is an integration constant. The axial force T in the tube at a station where $r = R$ is then

$$T = \frac{2\pi\sigma_1 Rt'}{\left[1+\left(\frac{\mathrm{d}r}{\mathrm{d}x}\right)^2\right]^{\frac{1}{2}}} = \pi EtR(p_0 - q^2 + \lambda), \tag{20}$$

where p_0 and q are the non-dimensionalized total pressure and flow rate, as in (2). If λ is eliminated from (19) and (20), and $\xi = x/R$, $d = t'/t$, $\sigma = \sigma_1/E$, $\tau = T/\pi EtR$, $\rho = r/R$ are used to non-dimensionalize there follows

$$\sigma = \frac{1}{2d\rho^3}[q^2 + (\tau - p_0 - q^2)\rho^2 + p_0\rho^4]\left[1 + \left(\frac{d\rho}{d\xi}\right)^2\right]^{\frac{1}{2}}. \tag{21}$$

Substituting (17) and (19) in (16*b*) yields σ_m; using this result and σ_1 from (19) in (16*c*) gives in a quadratic equation for d, which upon taking the proper root and non-dimensionalization gives

$$d = \frac{1}{2\rho^2}\left[\rho^2\{1 + \mu(1-\rho)\}\right.$$
$$\left. + \left[\{1 + \mu(1-\rho)\}^2\rho^4 - 2\mu(1+\mu)\rho\{q^2 + (\tau - p_0 - q^2)\rho^2 + p_0\rho^4\}\left\{1 + \left(\frac{d\rho}{d\xi}\right)^2\right\}^{\frac{1}{2}}\right]^{\frac{1}{2}}\right]. \tag{22}$$

Finally, using the expressions for σ_m, σ_1 and d, and (18) in the membrane formula (15) yields

$$\rho\{q^2 + (\tau - p_0 - q^2)\rho^2 + p_0\rho^4\}\frac{d^2\rho}{d\xi^2} + \rho(1-\rho)\left[\rho^2\{1 + \mu(1-\rho)\}\right.$$
$$\left. + \left(\{1 + \mu(1-\rho)\}^2\rho^4 - 2\mu(1+\mu)\rho\{q^2 + (\tau - p_0 - q^2)\rho^2 + p_0\rho^4\}\left\{1 + \left(\frac{d\rho}{d\xi}\right)^2\right\}^{\frac{1}{2}}\right)^{\frac{1}{2}}\right]$$
$$\times\left\{1 + \left(\frac{d\rho}{d\xi}\right)^2\right\}^{\frac{1}{2}} + \{-(2+\mu)q^2 - \mu(\tau - p_0 - q^2)\rho^2 + (2-\mu)p_0\rho^4\}$$
$$\times\left\{1 + \left(\frac{d\rho}{d\xi}\right)^2\right\} = 0, \tag{23}$$

which gives the shape of the tube for given total pressure, flow rate and axial force at $r = R$ (Reyn 1982). No *ad hoc* assumptions have been made so far, and (23) could be used for more accurate calculations. It includes the equation for uniform flows through inflated cylindrical tubes under axial tension, in which case there is the combined effect of the lateral contraction through Poisson's ratio already present in an unpressurized tube under tension, and an inflation by the pressure in the tube. In the problem to be studied in this paper the first effect can be accounted for by a τ-dependent correction of A_0 and t, and adjusting the boundary conditions arising from the requirement that the tube is held open at its ends. As may be seen later, such an adjustment will not change the variety of solutions of the boundary-value problem at hand and, for simplicity, we will refrain from doing so. Moreover, we shall use the approximation of the 'tube law' (6) for slightly inflated tubes by dropping the term containing μ. For these reasons, primarily to obtain a simpler equation, we put $\mu = 0$ in (23), which then, using (6) (with $\mu = 0$), may be written as

$$\rho\{q^2 + (\tau - p_0 - q^2)\rho^2 + p_0\rho^4\}\frac{d^2\rho}{d\xi^2} - 2\rho^4 P(\rho)\left\{1 + \left(\frac{d\rho}{d\xi}\right)^2\right\}^{\frac{1}{2}} + -2(q^2 - p_0\rho^4)\left\{1 + \left(\frac{d\rho}{d\xi}\right)^2\right\} = 0. \tag{24}$$

Although (24) is derived on the assumption, that the tube is axially symmetric it can be given a meaning for collapsible tubes since ρ and $P(\rho)$ are then also defined. In particular (24) includes (7), the equation for uniform flows through cylindrical tubes, also when the tube is collapsed and for $P(\rho)$ a tube law for collapsible tubes

is used. Therefore, as an approximation, (24) will also be used to determine the area variation of non-cylindrical collapsible tubes. Stated differently, (24) determines for a given total pressure, flow rate and axial force at $r = R$, the area variation of a tube with a, to some extent unrealistic, elastic structure, yet containing sufficient essential features to yield valuable qualitative information about real tube behaviour.

An attractive feature of (24) is that, to some extent, it can be integrated analytically so that a favourable starting point can be chosen for its numerical integration. Integration in the phase plane yields

$$\left\{1+\left(\frac{\mathrm{d}\rho}{\mathrm{d}\xi}\right)^2\right\}^{\frac{1}{2}} = \frac{C\rho^2 - 2\rho^2\int_1^\rho \alpha P(\alpha)\,\mathrm{d}\alpha}{q^2+(\tau-p_0-q^2)\rho^2+p_0\rho^4}, \tag{25}$$

where C is an integration constant. Further integration gives

$$\xi = \xi_0 + \int_{\rho(\xi_0)}^{\rho} \frac{\{q^2+(\tau-p_0-q^2)\rho^2+p_0\rho^4\}\,\mathrm{d}\rho}{\left[\rho^4\left\{C+2\int_1^\rho \alpha P(\alpha)\,\mathrm{d}\alpha\right\}^2 - \{q^2+(\tau-p_0-q^2)\rho^2+p_0\rho^4\}^2\right]^{\frac{1}{2}}} \tag{26}$$

for the shape of the tube. Even if simple analytic expressions for the tube law are used, there can be little hope that (26) can be evaluated in terms of elementary functions. However, it can be used as a starting point for numerical calculations. In the phase plane, with $\rho = \rho(s)$, $\mathrm{d}\rho/\mathrm{d}\xi = y = y(s)$, (24) can be written as the system

$$\left.\begin{aligned} \frac{\mathrm{d}\rho}{\mathrm{d}s} &= \{q^2+(\tau-p_0-q^2)\rho^2+p_0\rho^4\}\rho y, \\ \frac{\mathrm{d}y}{\mathrm{d}s} &= 2\rho^4 P(\rho)\{1+y^2\}^{\frac{1}{2}} + 2(q^2-p_0\rho^4)(1+y^2). \end{aligned}\right\} \tag{27}$$

Various qualitatively different phase portraits that may occur are sketched in figure 2; the arrows point in the direction of increasing ξ. Phase portraits are symmetric with respect to the ρ-axis. Equilibrium points are given by the solutions of

$$p_0\rho^4 - \rho^4 P(\rho) - q^2 = 0, \quad y = 0, \tag{28}$$

which represent the uniform flows in cylindrical tubes discussed in the preceding section. For $q = 0$, in addition, the y-axis also consists of equilibrium points. Near simple equilibrium points (in $\rho = \rho_i$, $y = 0$) (27) may be linearized to yield, with $\bar{\rho} = \rho - \rho_i$, $\bar{y} = y$,

$$\left.\begin{aligned} \frac{\mathrm{d}\bar{\rho}}{\mathrm{d}s} &= \{q^2+(\tau-p_0-q^2)\rho_i^2+p_0\rho_i^4\}\rho_i\bar{y}, \\ \frac{\mathrm{d}\bar{y}}{\mathrm{d}s} &= 2\frac{\mathrm{d}}{\mathrm{d}\rho}\{q^2+\rho^4P(\rho)-p_0\rho^4\}\big|_{\rho=\rho_i}\bar{\rho}. \end{aligned}\right\} \tag{29}$$

When the wave speed is non-dimensionalized and (9) is used there follows

$$c = \frac{C}{\left(\frac{Et}{\rho_f R}\right)^{\frac{1}{2}}} = (\tfrac{1}{2}\rho P'(\rho))^{\frac{1}{2}}. \tag{30}$$

With the use of (10), (21), (28) and (30), the eigenvalues of the coefficient matrix of (29) may then be found:

$$\lambda_{1,2} = \pm 2\rho_i^3 c_i\{2\sigma_i(1-S_i^2)\}^{\frac{1}{2}}. \tag{31}$$

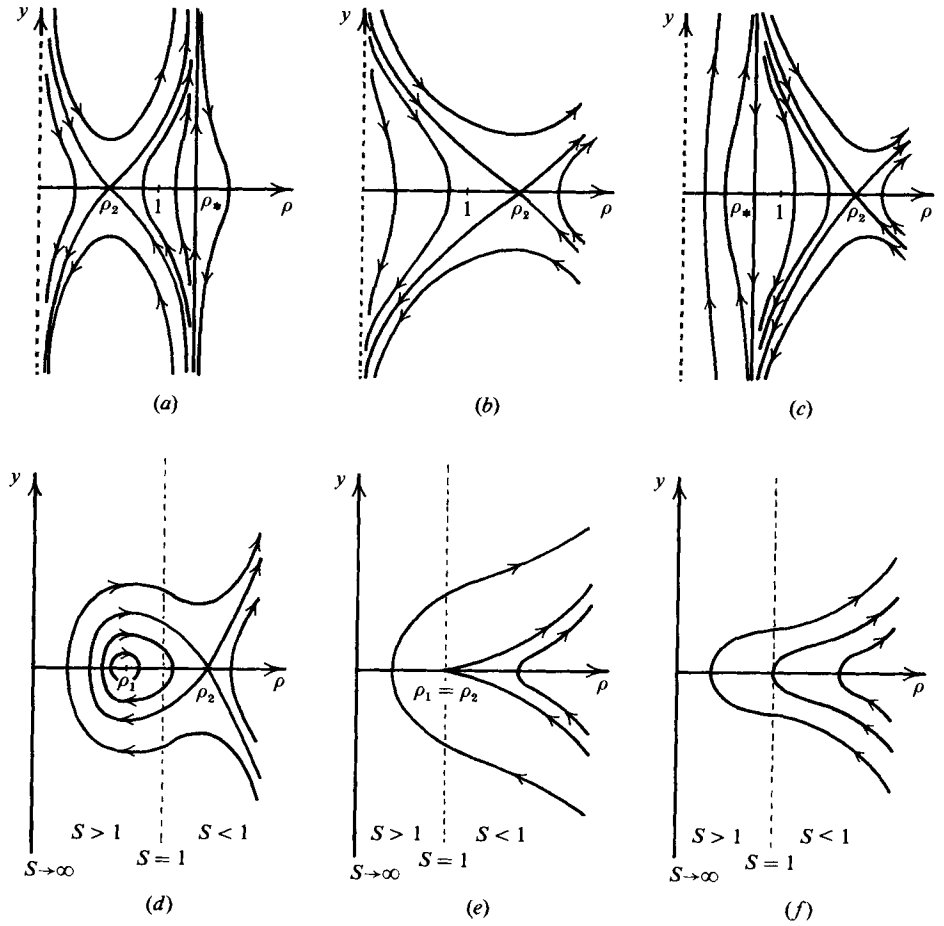

FIGURE 2. Types of phase portraits with variables ρ and $y = \mathrm{d}\rho/\mathrm{d}\xi$. (*a*) $q = 0$, $p_0 < 0 < \tau$; (*b*) $q = 0$, $0 \leqslant p_0 < \tau$; (*c*) $q = 0$, $0 < \tau < p_0$; (*d*) $0 < q < q_E$; (*e*) $q = q_E$; (*f*) $q > q_E$.

Phase portraits for no flow are given in figure 2(*a–c*). There is one equilibrium point on the ρ-axis if $p_0 = P(\rho_i)$ has a unique solution for ρ_i, which is true for common tube laws. If, furthermore, $P(\rho) \lessgtr 0$ for $\rho \lessgtr 1$, then $\rho_i (= \rho_2) \lessgtr 1$ for $p_0 \lessgtr 0$, and with (21) it may be seen that $\sigma_i (= \sigma_2) > 0$ if $\tau > 0$. As a result, (31) shows that the equilibrium point is a saddle point. It corresponds to the cylinder-type solution. Other types of solution are those showing somewhere along the tube a minimal (maximal) area of the tube and a continuous widening (narrowing) of the tube away from it, and also solutions with a continuous widening or narrowing all along the tube. These solutions eventually either enter a region where the tube is highly collapsed or highly inflated and the applicability of the theory is doubtful, or approach the solution given by $\rho(s) \equiv \rho_* = \{1 - (\tau/p_0)\}^{\frac{1}{2}}$, in which case the tube ends with this radius though with an infinite slope. The occurrence of the solution $\rho = \rho_*$ points to the phenomenon that elastically unstable solutions appear, representing (membrane-like) tubes supporting compression forces. For example, in figure 2(*a*) the case $p_0 < 0$, $\tau > 0$ is illustrated, and the solutions in the region $\rho > \rho_*$ are of such a type; on these solutions $\sigma < 0$ as follows from (21). The solution $\rho \equiv \rho_*$ corresponds to the case that the tube is degenerated into one of zero length. Solutions near it correspond to very short tubes

supporting the overpressure either by tensile stresses on an inwardly bent tube or by compression stresses in an outwardly bent tube. A similar discussion can be given for the case $0 < \tau < p_0$, which is illustrated in figure 2(*c*); for the case $0 \leqslant p_0 < \tau$ the phenomenon does not occur, as may be seen in figure 2(*b*). The phenomenon may also occur if there is flow in the tube. However, we shall avoid solutions with $\sigma < 0$, since they are not of much practical interest. As follows from (21), there is for all values of the parameters a strip around $\rho = 1$ in the phase plane, where $\sigma > 0$ for $\tau > 0$, and we shall restrict our attention to such a strip (which possibly also may extend over $0 < \rho < \infty$). In figure 2(*d*) the case $0 < q < q_E$ is illustrated. It corresponds to the case that (28), (7) has two solutions $\rho_1 < \rho_2$ (region II in figure 1). Since $S_1 > 1$ and $S_2 < 1$, and $\sigma_i > 0$ ($i = 1, 2$), it follows from (31) that ρ_1 is a centrepoint and ρ_2 is a saddle point. From (4), (10) follows that $S \to \infty$ as $\rho \to 0$, and from (10) with $\{P(\rho) + \frac{1}{4}\rho P(\rho)\}' > 0$ that S decreases monotonically with ρ; there is thus a unique line $\rho \equiv$ constant between the centrepoint and the saddle point on which $S = 1$, and $S > 1$ for smaller values of ρ, $S < 1$ for larger values of ρ. The closed curves inside the separatrix loop represent tube shapes that are periodic with a wavelength approaching infinity as the loop is approached. They contain flow that is supercritical in part or over the full length of the tube. Other solutions show a minimum tube area at some point of the tube and a continuous widening of the tube with distance away from that point; solutions near the separatrix loop represent tubes of which a portion is convex outwards, while the rest is concave outwards. Solutions to the right of the saddle point correspond to subcritical flow; solutions surrounding the separatrix loop correspond also to supercritical flow in the region around the minimum tube area. Near an equilibrium point (24) has the linearized form

$$\rho_i \sigma_i \frac{\mathrm{d}^2\rho}{\mathrm{d}\xi^2} + 2c_i^2(S_i^2 - 1)(\rho - \rho_i) = 0, \tag{32}$$

from which the wavelength of periodic solutions may be derived at $\rho_i = \rho_1$ (the centrepoint, then $S_1 > 1$), given by

$$L = \frac{\pi(2\rho_1 \sigma_1)^{\frac{1}{2}}}{c_1(S_1^2 - 1)^{\frac{1}{2}}}. \tag{33}$$

A similar expression was given by McClurken *et al.* (1981) in their study of steady, supercritical flow in collapsible tubes. A linearized analysis of inviscid wave propagation in nearly cylindrical collapsed tubes yields for the wavelength of standing waves in a steady flow (McClurken *et al.* (1981), formula (27), p. 402) in our notation

$$L = \frac{\pi(2\rho_1 \sigma_1)^{\frac{1}{2}}}{c_1(S_1^2 - 1)^{\frac{1}{2}}} \frac{\rho_1^{\frac{1}{2}}}{(1 - \rho_1^2)^{\frac{1}{4}}}, \tag{34}$$

which differs from (33) by the factor $\rho_1^{\frac{1}{2}}(1 - \rho_1^2)^{-\frac{1}{4}}$, undoubtedly as a result of the different tube model used by McClurken *et al.* (1981). Although comparison of measured and theoretical wavelengths (figure 5 in McClurken *et al.*) leads to an agreement which is called most satisfactory by the authors, use of (30) may very well improve this agreement in particular near $\rho_1 = 1$. (In a comparison with numerical calculations, taking friction into account, and given in figure 11 of McClurken *et al.* (1981), (34) is used with the factor $(1 - \rho_1^2)^{\frac{1}{4}}$ omitted.) Unfortunately, the experimental results are not presented in enough detail to allow comparison with (33). In figure 2(*e*) the case $q = q_E$ is illustrated. It corresponds to flow limitation in the cylindrical uniform-flow solution which is now represented by a higher-order equilibrium point (cusp point in $\rho_1 = \rho_2$). Solutions completely to the right of the cusp

point correspond to subcritical flow; the other solutions correspond also to supercritical flow in a region of the tube near the minimum tube area. Finally, in figure 2(*f*) $q > q_E$ is illustrated. There are no equilibrium points, so flow through a cylindrical tube is impossible, but there exist solutions with a minimum tube area somewhere along the tube and a widening of the tube away from it.

4. Steady flow through a collapsible tube held open at the ends. Flow limitation in non-cylindrical tubes

We shall now consider the steady, incompressible, inviscid flow through a collapsible tube held open at the ends. Finding the streamwise area distribution of the tube for a given total pressure p_0, flow rate q and pulling force τ amounts to solving a two-point boundary-value problem for (24) with boundary conditions $\rho(-l) = \rho(l) = 1$, so that the tube extends from $\xi = -l$ to $\xi = l$. Obviously, a solution of this boundary-value problem will be represented in the phase plane by a segment of an integral curve, connecting intersection points thereof with the line $\rho \equiv 1$. For example, in figure 3(*a*) the segment LU is shown, connecting, in the direction of increasing ξ, the lower point L on $\rho \equiv 1$ with the upper point U, and since all along the integral curve $\rho < 1$, LU represents a collapsed tube with a certain length l_{LU}. With (26), and since the phase portrait is symmetric around the ρ-axis, then

$$l_{LU} = 2\int_{\rho_{\min}}^{1} \frac{\{q^2 + (\tau - p_0 - q^2)\rho^2 + p_0\rho^4\}\,\mathrm{d}\rho}{\left[\rho^4\left(C + 2\int_1^{\rho} \alpha P(\alpha)\,\mathrm{d}\alpha\right)^2 - \{q^2 + (\tau - p_0 - q^2)\rho^2 + p_0\rho^4\}^2\right]^{\frac{1}{2}}}, \tag{35}$$

where C for a given $\rho_{\min}$ may be determined from (25) by putting $y = 0$. Similarly, an integral-curve segment UL represents an inflated axially symmetric tube of length l_{UL}, for which, with (26), it follows that

$$l_{UL} = 2\int_{1}^{\rho_{\min}} \frac{\{q^2 + (\tau - p_0 - q^2)\rho^2 + p_0\rho^4\}\,\mathrm{d}\rho}{\left[\rho^4\left(C + 2\int_1^{\rho} \alpha P(\alpha)\,\mathrm{d}\alpha\right)^2 - \{q^2 + (\tau - p_0 - q^2)\rho^2 + p_0\rho^4\}^2\right]^{\frac{1}{2}}}, \tag{36}$$

where C may be found for a given $\rho_{\max}$. Solutions to the boundary-value problem will be sought in an indirect way by considering the effects of variation of the parameters on tube lengths, corresponding to integral-curve segments LU, UL and possible combinations of them. The number of solutions for a given tube length then follows by cross-plotting. Except in some special cases, the dependence of l_{LU} and l_{UL} on the parameters can only be traced by numerical calculations. Such calculations were made by Reyn & Bakker (1984) for a set of values of p_0 and q^2, and $\tau = 0.6$ (with one exception, wherein τ is varied), which roughly corresponds to a relative strain of 30%. (The measurements by Lyon *et al.* (1981) are made on collapsible tubes stretched up to 100%.) For a collapsed part of the tube ($\rho < 1$), tube law (5) was used with $\beta = 0.001$, which corresponds to a wall thickness/tube radius ratio of about 0.1. For an inflated part ($\rho > 1$) tube law (6) was used with $\mu = 0$. For each selected pair of values for p_0 and q^2 the functions $l_{LU}(\rho_{\min})$ and/or $l_{UL}(\rho_{\max})$ were calculated. From this is determined how many solutions for a given tube length $2l$ are possible. For example, figure 3(*a*) corresponds to $p_0 < 0$, $q^2 = 0$, and calculations over a range of values of p_0 from -0.005 to -0.12 indicate a monotonically decreasing function $l_{LU}(\rho_{\min})$ on the interval $\rho_2 < \rho_{\min} < 1$. Furthermore from (35) it follows that $l_{LU} \to \infty$ as $\rho_{\min} \to \rho_2$ and $l_{LU} \to 0$ as $\rho_{\min} \to 1$. It is then concluded that the boundary-value

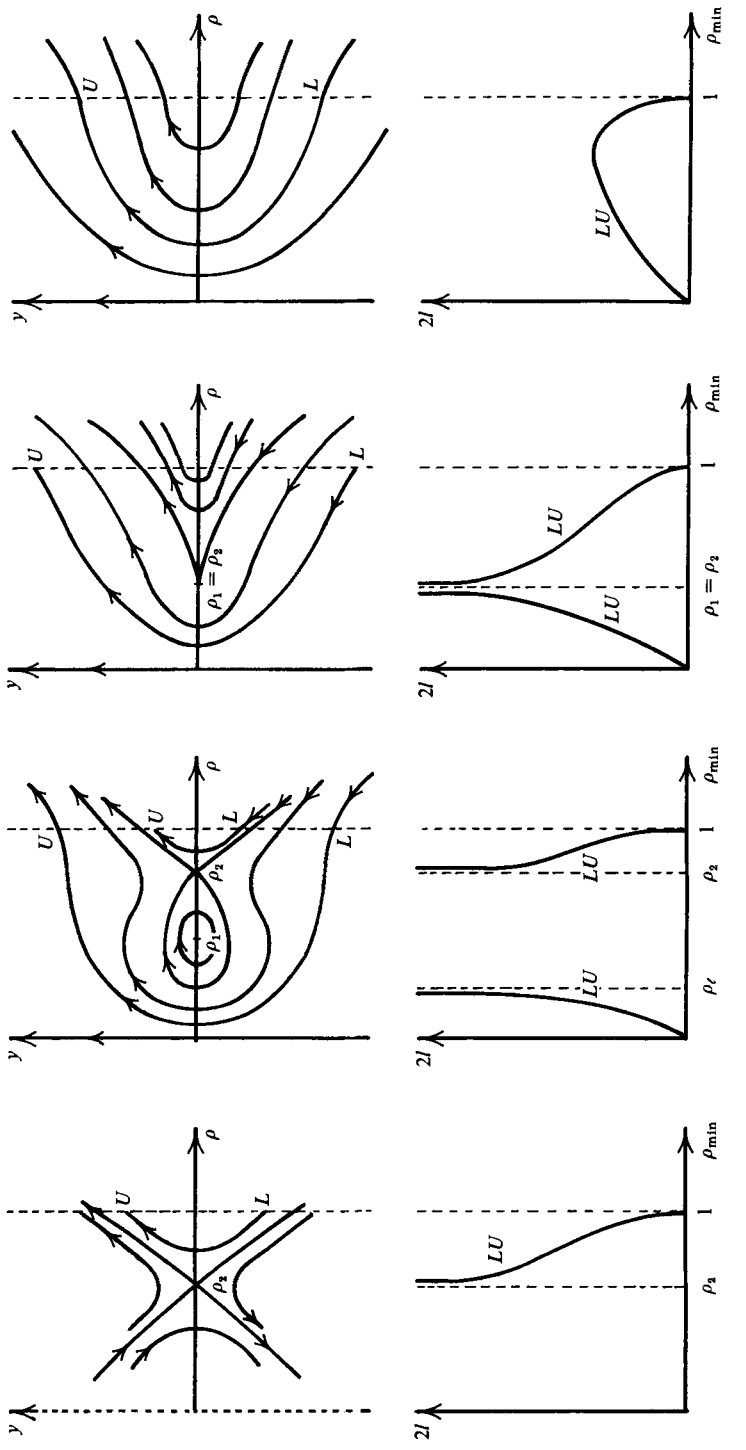

FIGURE 3. Phase trajectories and corresponding tube lengths for negative total pressures. (*a*) $q = 0$; (*b*) $0 < q < q_E$; (*c*) $q = q_E$; (*d*) $q > q_E$.

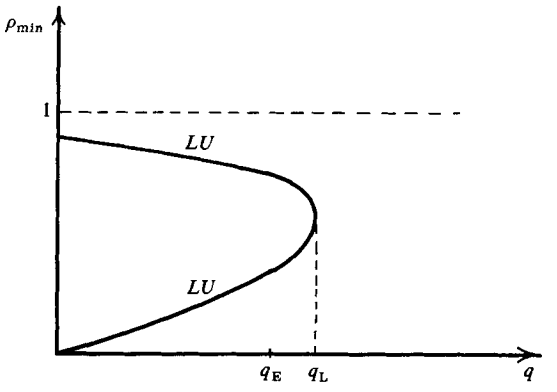

FIGURE 4. Bifurcation diagram for a given tube length and negative total pressure.

problem has a unique solution for all tube lengths $0 < 2l < \infty$. It should be emphasized that this conclusion does not rest on a mathematically tied proof for all parameter values and possible tube laws, but merely on numerical evidence for some choices of numerical values for these parameters. A general statement about the solution of the boundary-value problem will therefore be avoided, showing in the first place how complicated the answer is for more or less representative values of the parameters. In order to study also the process of flow limitation, the presentation will be made with an emphasis on changing the flow rate for a given total pressure. Because of the different character of this process a division is made into three cases: (i) negative and zero total pressure; (ii) positive subcritical and critical total pressure; (iii) positive supercritical total pressure. The division of positive total pressure is connected with the discussion of steady flow through cylindrical tubes given in §2 and illustrated in figure 1. Under the conditions made with respect to the tube law, there are two (possibly coincident) or none such flows for a given total pressure, among which there is exactly one solution $\rho \equiv 1$ if $p_0 > 0$. A (positive) total pressure will then be called subcritical, critical or supercritical if the flow in the tube $\rho \equiv 1$ at that total pressure is subcritical, critical or supercritical, respectively. In the context of §2 this means $0 < p_0 < \frac{1}{4}P'(1)$, $p_0 \equiv \frac{1}{4}P'(1)$, $\frac{1}{4}P'(1) < p_0$, respectively.

4.1. *Negative and zero total pressure*

In figure 3 phase trajectories are sketched that may represent solutions of the boundary-value problem. They are characterized by $\rho_{\min}$, their intersection point with the ρ-axis, and their corresponding tube length $l_{LU} = 2l$ is sketched as a function of $\rho_{\min}$. They are based on numerical calculations for $p_0 = -0.1$, $q^2 = 0.0002$ to 0.02, and $q^2 = 0$, $p_0 = -0.005$ to -0.12. Under no-flow conditions (figure 3*a*) a unique solution is apparent for all tube lengths, $0 < 2l < \infty$, and the tube is collapsed over its full length. In figure 3(*b*) it is shown that a slight increase in flow rate causes a centrepoint and a separatrix loop to arise in the phase plane and an additional (highly) collapsed solution surrounding the separatrix loop appears, represented by l_{LU} ($\rho_{\min}$) on $0 < \rho_{\min} < \rho_\ell$, where ρ_ℓ is the intersection point of the separatrix loop with the ρ-axis. As a result, there are now two solutions for all tube lengths $0 < 2l < \infty$, both collapsed over the full length of the tube. The solution completely to the right of ρ_2 is subcritical, whereas the other one is also subcritical except for a supercritical region around the minimum area of the tube. For $q = q_E$ (figure 3*c*) the centrepoint and saddle point coincide to form a cusp point and the separatrix

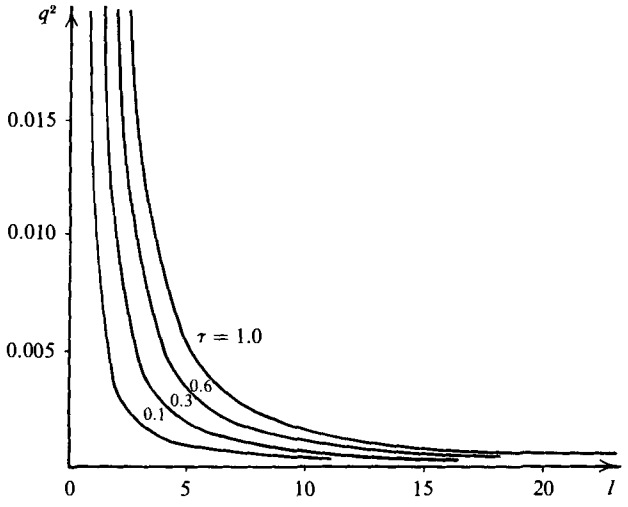

FIGURE 5. Flow-limitation values of the flow rate for various values of τ; $p_0 = 0$.

loop has shrunk to one point; $\rho_\ell = \rho_1 = \rho_2 < 1$. For cylindrical tubes, increase of the flow rate cannot occur since q_E is the flow limitation flow rate. For tubes held open at the ends there are, for all tube lengths, two (collapsed) solutions at $q = q_E$, which, for a given tube length, disappear after a coalescence if q is increased sufficiently (figure 3*d*). In figure 4 the bifurcation diagram for a given tube length and negative total pressure is given, where the solutions are characterized by the value of ρ_{min} and $q_L > q_E$ is the flow rate at flow limitation in the finite tube. The case $p_0 = 0$ does not differ very much from $p_0 < 0$; only figure 3(*a*) changes in that now $\rho_2 = 1$, and, trivially, there is a unique solution $\rho \equiv 1$ of the boundary-value problem. Calculations for $p_0 = 0$ were made with q^2 ranging from 0 to 0.02. The effect of changes in τ on the process of flow limitation for $p_0 = 0$ was investigated by calculating the flow rate at flow limitation as a function of tube length for various values of τ. The effect of shortening the tube on postponing flow limitation is clearly visible in figure 5, which also shows that increasing the tension for a given tube length also postpones flow limitation.

4.2. *Positive subcritical and critical total pressures*

In figure 6 phase trajectories and corresponding tube lengths for positive subcritical total pressures are sketched. They are based on numerical calculations for $p_0 = 0.00075$, $q^2 = 0$ to 0.0007; $p_0 = 0.15$, $q^2 = 0$ to 0.12. If there is no flow, (figure 6*a*), the result is similar to that for $p_0 < 0$: there is a unique solution for all tube lengths $0 < 2l < \infty$, the difference being that the tube is now inflated and represented by a segment UL of an integral curve in the phase plane. Curve segments UL are characterized by the value of ρ_{max}, corresponding to the maximum area of the tube for that solution. Figure 6(*b*) shows that a slight increase in flow rate causes a centrepoint and a separatrix loop to arise in the phase plane, as for $p_0 < 0$. The line $\rho \equiv 1$, however, now intersects the separatrix loop and intersects the ρ-axis between the centrepoint and the saddle point. As a result solution-curve segments LU representing collapsed tubes appear in addition to the inflated solutions of type UL. If U and L are selected to coincide on the ρ-axis, the LU segment forms a closed curved in the phase plane and the tube extends over one wavelength $\mathscr{L}_1$ of a periodic solution with $\rho_{max} = 1$. It is found that, if L and U are moved along $\rho \equiv 1$ and away from

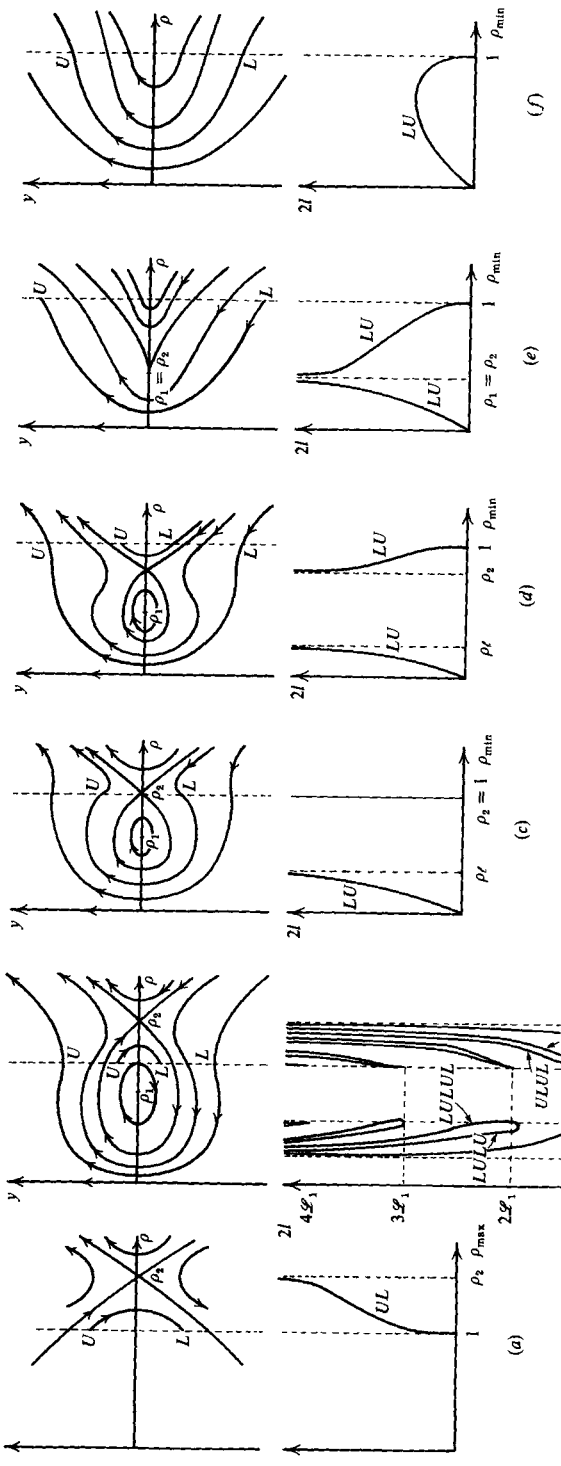

FIGURE 6. Phase trajectories and corresponding tube lengths for (positive) subcritical total pressures. (*a*) $q = 0$; (*b*) $0 < q < p_0^{\frac{1}{2}}$; (*c*) $q = p_0^{\frac{1}{2}}$; (*d*) $p_0^{\frac{1}{2}} < q < q_E$; (*e*) $q = q_E$; (*f*) $q > q_E$.

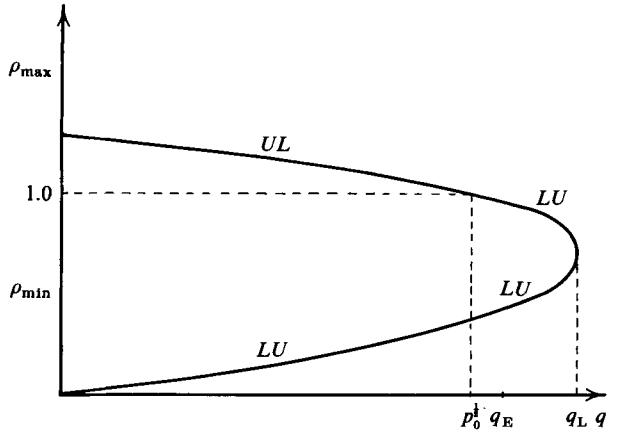

(*a*)

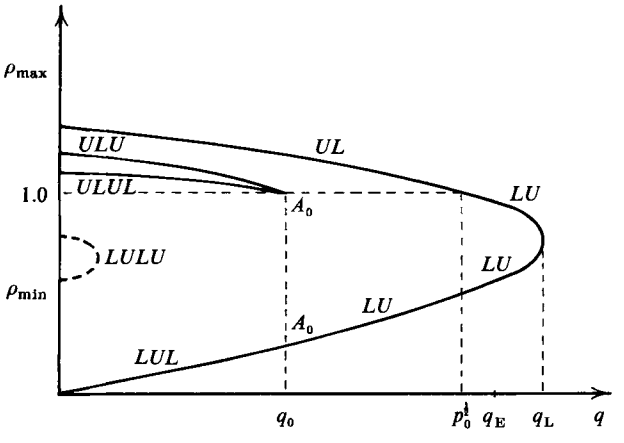

(*b*)

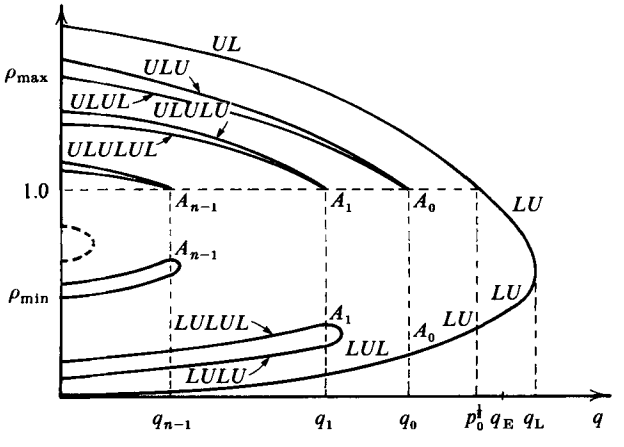

(*c*)

FIGURE 7. Bifurcation diagrams for a given tube length and (positive) subcritical total pressures. (*a*) $0 < 2l < \mathscr{L}_1(0)$; (*b*) $\mathscr{L}_1(0) < 2l < 2\mathscr{L}_1(0)$; (*c*) $n\mathscr{L}_1(0) < 2l < (n+1)\mathscr{L}_1(0)$.

the ρ-axis, the tube length then decreases monotonically, going to zero for U, L going to infinity. Integral-curve segments inside the saddle-to-saddle loop may be extended with other LU and/or UL segments, so that the solution then overlaps with one or more wavelengths of a periodic solution. For tubes that start with a collapsed part there are the possibilities LU, LUL, $LULU$, ..., and for tubes starting with an inflated part UL, ULU, $ULUL$, ... Solutions indicated with an odd number of letters correspond to tube lengths that are an integer multiple of the wavelength of a periodic solution; if this multiple is n, then such a situation occurs for $2n+1$ letters. The solutions LUL and ULU, $LULUL$ and $ULULU$, ... are pairwise related in that the transformation $\xi \to -\xi$ (or flow reversal) transforms one into the other. The solutions with an even number of letters represent tubes that are symmetric in ξ. A sketch of the variation of the tube length $2l$ for various types of solution is given in figure 6(*b*). For solutions starting with a collapsed part, $2l$ is given as a function of $\rho_{\min}$ and for those starting with an inflated part as a function of $\rho_{\max}$. In drawing this figure, it is assumed that the wavelength of a periodic solution increases monotonically with the 'amplitude' $= \rho_{\max} - \rho_{\min}$; it has the value $\mathscr{L}_1$ for $\rho_{\max} = 1$ and ∞ for $\rho_{\max} = \rho_2$. (The numerical calculations indicate that for some values of the parameters this monotonicity is lost on part of the interval; however, we shall not discuss the additional complications arising in that case.) As a result, the curves for LUL, ULU, $LULUL$, $ULULU$, ... are monotonic, and since UL is monotonic, the curves for $ULUL$, $ULULUL$, $ULULULUL$, ... are also monotonic. The monotonicity of LU, however, does not lead to the same conclusion for $LULU$, $LULULU$, $LULULULU$, ..., since the curve LU has a vertical tangent at $2l = \mathscr{L}_1$ and the curve LUL has not. From figure 6(*b*) it may be seen that the number of solutions of the boundary-value problem increases in a piecewise-constant manner with the tube length, and is at least $4n$, where n is the integer number of times that $\mathscr{L}_1$ is included in the tube length. This effect also occurs when the flow rate is increased only slightly above zero, since with (35) it may be shown that $\mathscr{L}_1$ has a finite limit (not equal to zero) for $q \to 0$. If $q \to p_0^{\frac{1}{2}}$ (figure 6*c*), the saddle point ρ_2 has moved to $\rho = 1$, and $\mathscr{L}_1 \to \infty$. For all tube lengths $0 < 2l < \infty$ only two solutions are left: a collapsed solution LU and the solution $\rho \equiv 1$. Further increase of q yields the sequence given in figure 6(*d–f*), which is similar to the sequence in figure 3(*b–d*) for $p_0 < 0$, and the flow-limitation process takes place as for $p_0 \leqslant 0$.

Bifurcation diagrams for given tube lengths and total pressure and varying flow rates may now be drawn on the basis of figure 6, and are sketched in figure 7 for various tube lengths. Tube lengths are measured in units of $\mathscr{L}_1(0)$; where $\mathscr{L}_1(q)$ is the wavelength of a periodic solution with $\rho_{\max} = 1$ for a flow rate $q < p_0^{\frac{1}{2}}$ The situation for $0 < 2l < \mathscr{L}_1(0)$ is given in figure 7(*a*). For $q = 0$ there is one solution, an inflated one (UL) and indicated by its value of $\rho_{\max}$, whereas for a slightly higher q, a collapsed solution (LU) also appears, indicated by its value of $\rho_{\min}$. On increasing q to $p_0^{\frac{1}{2}}$ the UL solution merges into the solution $\rho(\xi) \equiv 1$ and further increase leads to two collapsed solutions which, at the flow-limitation value q_L, merge ($q_L > q_E$). Figure 7(*a*) is similar to figure 4 for $p_0 < 0$.

The situation for $\mathscr{L}_1(0) < 2l < 2\mathscr{L}_1(0)$ is given in figure 7(*b*). Again, there is one (inflated) solution UL for $q = 0$. Increase of q now leads to the addition of the periodic solutions ULU and LUL and the symmetric solution $ULUL$ and, depending on a more detailed knowledge of the tube length, possibly also to two symmetric solutions of the type $LULU$, which disappear after mergence at some higher flow rate. At a still higher flow rate $q = q_0$, the three solutions ULU, LUL and $ULUL$ merge into one solution A_0, which extends over one wavelength of a periodic solution with

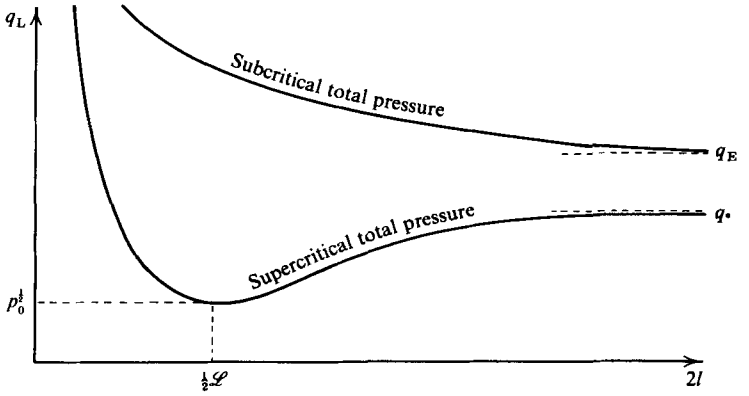

FIGURE 8. Flow-limitation values of the flow rate as a function of tube length.

wavelength $\mathscr{L}_1 = 2l$ (and $\rho_{\max} = 1$). For $q > q_0$ this solution changes into a collapsed one LU and the rest of the process is the same as sketched in figure 7 (*a*), but with a smaller value of q_L ($> q_E$) since the tube is longer. For $n\mathscr{L}_1(0) < 2l < (n+1)\mathscr{L}_1(0)$ the situation as sketched in figure 7 (*c*) prevails. Again there is one (inflated) solution UL for $q = 0$. Increase of q now leads to the addition of $2n$ periodic solutions

$$ULU,\ LUL,\ \ldots,\ \underbrace{ULU\ldots U}_{2n+1},\ \underbrace{LUL\ldots L}_{2n+1},$$

and $2n-1$ symmetric solutions

$$ULUL,\ \ldots,\ \underbrace{LU\ldots U}_{2n},\ \underbrace{UL\ldots L}_{2n+2},$$

and possibly also to two symmetric solutions of the type

$$\underbrace{LU\ldots U}_{2n+2},$$

which disappear after mergence at some higher flow rate. At a still higher flow rate $q = q_{n-1}$, the solutions

$$\underbrace{ULU\ldots U}_{2n+1},\ \underbrace{LUL\ldots L}_{2n+1} \quad \text{and} \quad \underbrace{UL\ldots L}_{2n+2}$$

merge into one solution A_{n-1}, which extends over n wavelengths of a periodic solution with wavelength $\mathscr{L}_1(q_{n-1})$ (and $\rho_{\max} = 1$). For $q > q_{n-1}$, this solution changes into a symmetric one

$$\underbrace{LU\ldots U}_{2n}$$

which merges with the other solution of type

$$\underbrace{LU\ldots U}_{2n}$$

at a higher flow rate. This process is repeated at the flow rates $q = q_{n-2}, q_{n-3}, \ldots, q_1$ at which the solutions $A_{n-2}, A_{n-3}, \ldots, A_1$ exist, being solutions which extend over $n-1, n-2, \ldots, 2$ wavelengths of a periodic solution with wavelength $\mathscr{L}_1(q_i)$ (and $\rho_{\max} = 1$) respectively, where $i = n-2, n-3, \ldots, 1$ respectively. Finally, for some $q > q_1$ all solutions have disappeared, except for the ones also discussed in relation to figure 7 (*b*), and the process continues as in that figure with smaller q_I, since again the tube is longer than in the previous case. The process may be viewed as a sequence

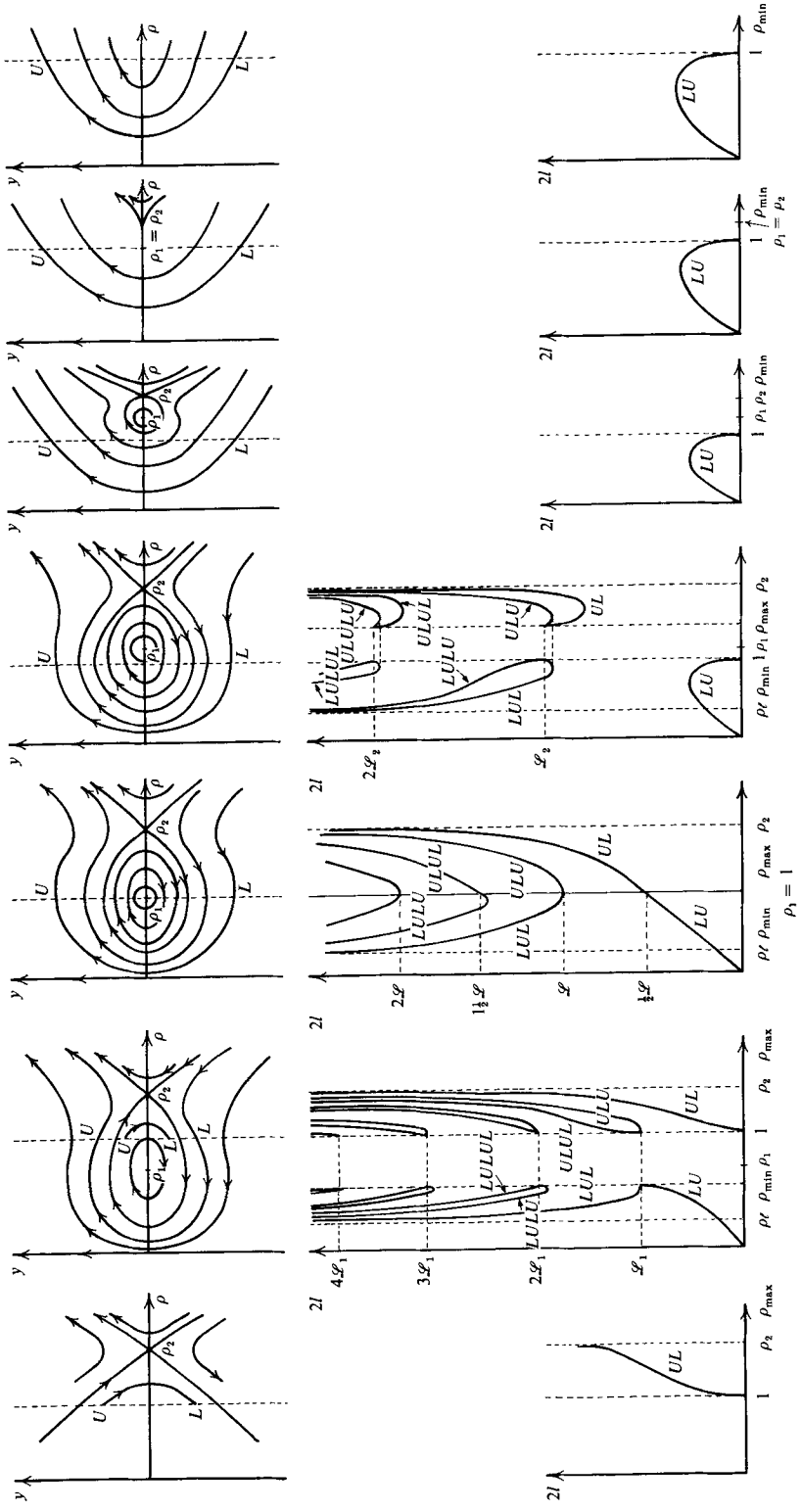

FIGURE 9. Phase trajectories and corresponding tube lengths for (positive) supercritical total pressures. (*a*) $q = 0$; (*b*) $0 < q < p_0^{\frac{1}{2}}$; (*c*) $q = p_0^{\frac{1}{2}}$; (*d*) $p_0^{\frac{1}{2}} < q < q_*$; (*e*) $q_* < q < q_E$; (*f*) $q = q_E$; (*g*) $q > q_E$.

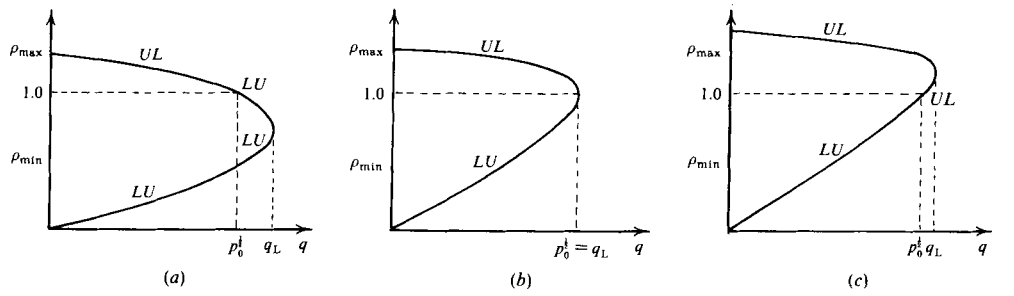

FIGURE 10. Bifurcation diagrams for a given tube length and (positive) supercritical total pressures; $0 < 2l < \mathscr{L}_1(0)$. (*a*) $0 < 2l < \frac{1}{2}\mathscr{L}$; (*b*) $2l = \frac{1}{2}\mathscr{L}$; (*c*) $\frac{1}{2}\mathscr{L} < 2l < \mathscr{L}$.

of flow limitations of higher order with the final flow limitation indicated as that of first order. Note that all flow limitations occur in tubes that start with a collapsed part and that shortening the tube postpones flow limitation as for negative and zero total pressure. The qualitative features of figure 5 ($p_0 = 0$) may thus again be recognized in the curve for subcritical total pressure in figure 8.

For (positive) critical total pressure, $q_E = p_0^{\frac{1}{2}}$, and the only difference with subcritical total pressure is that now figures 6(*c–e*) coincide with one figure like figure 6(*e*), with $\rho_1 = \rho_2 = 1$, and with the curve LU replaced by $\rho \equiv 1$. As a result it may be concluded that there is no qualitative difference with subcritical total pressure.

4.3. *Positive supercritical total pressures*

In figure 9 phase trajectories and corresponding tube lengths for positive supercritical total pressures are sketched. They are based on numerical calculations for $p_0 = 0.15$, $q^2 = 0$ to 0.30 and for $p_0 = 0.625$, $q^2 = 0$ to 1.25. For $0 \leqslant q < p_0^{\frac{1}{2}}$ there is no difference with subcritical total pressure; figures 9(*a,b*) are identical with figure 6(*a,b*) respectively. In contrast, however, figure 9(*c*) shows that if $q \to p_0^{\frac{1}{2}}$, the centrepoint ρ_1 has moved to $\rho = 1$, and $\mathscr{L}_1 \to \mathscr{L}$, where $\mathscr{L}$ is the wavelength of a periodic solution at the centrepoint if $\rho = 1$, $q = p_0^{\frac{1}{2}}$, which with (10), (21), (30) and (33), may be given by

$$\mathscr{L} = \frac{\pi(2\tau)^{\frac{1}{2}}}{2(p_0 - \frac{1}{4}P'(1))^{\frac{1}{2}}}. \tag{37}$$

With further increase of q the centrepoint crosses the line $\rho = 1$ and the situation is as in figure 9(*d*). Figure 9(*b–d*) have been drawn, using the same observations as given previously. Since, however, if $P(1) = 0$, $q = p_0^{\frac{1}{2}}$, $p_0 > 0$, the function $\rho(\xi) \equiv 1$ is an exact solution, nearby solutions may be obtained in a mathematically strict sense using the Lyapunov–Schmidt method (Reyn & Besjes 1984). Figure 9(*b–d*) include information obtained in this way. It was assumed, as in §2, that $P(1) = 0$, $P'(\rho) > 0$, $\{P(\rho) + \frac{1}{4}\rho P'(\rho)\}' > 0$, and $\tau > 0$. In figure 9(*d*) $\mathscr{L}_2$ is the wavelength of a periodic solution with $\rho_{min} = 1$, and $\mathscr{L}_2 \to \mathscr{L}$ as $q \to p_0^{\frac{1}{2}}$. If q is increased further above $p_0^{\frac{1}{2}}$, the separatrix loop moves to the right until, for some flow rate $q = q_*$, the line $\rho \equiv 1$ intersects the loop, at the ρ-axis; then $\mathscr{L}_2 = \infty$, and only solutions LU remain if $q > q_*$, as is sketched in figure 9(*e–g*). Bifurcation diagrams for given tube lengths, (positive) supercritical total pressures and varying flow rates may now be drawn on the basis of figure 9; however, apart from $\mathscr{L}_1(0)$ $\mathscr{L}$ should also be used to measure the tube length. For $0 < 2l < \mathscr{L}_1(0)$ figure 10(*a–c*) gives diagrams for $0 < 2l < \frac{1}{2}\mathscr{L}$, $2l = \frac{1}{2}\mathscr{L}$, $\frac{1}{2}\mathscr{L} < 2l < \mathscr{L}$ respectively. For $0 < 2l < \frac{1}{2}\mathscr{L}$, figure 10(*a*) shows that there is almost no difference with subcritical total pressure, as illustrated in figure 7(*a*),

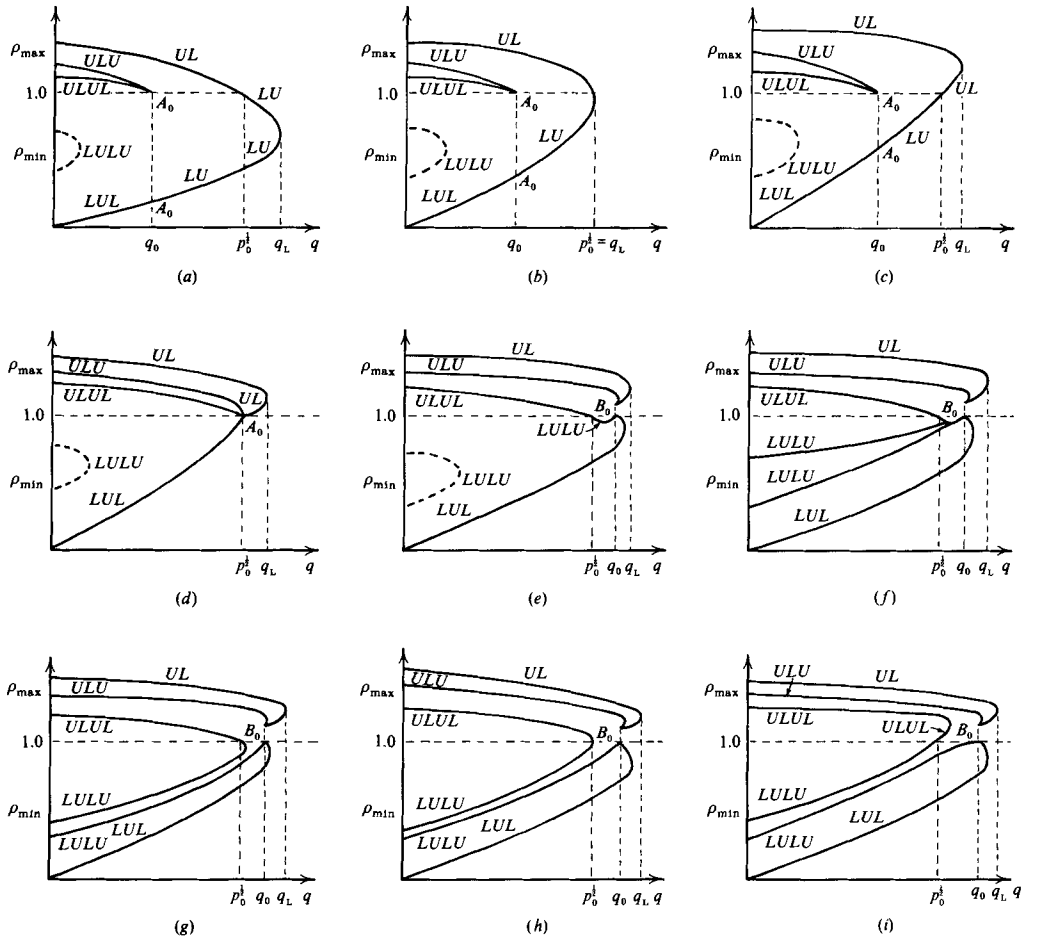

FIGURE 11. Bifurcation diagrams for a given tube length and (positive) supercritical total pressures, $\mathscr{L}_1(0) < 2l < 2\mathscr{L}_1(0)$. (*a*) $0 < 2l < \frac{1}{2}\mathscr{L}$; (*b*) $2l = \frac{1}{2}\mathscr{L}$; (*c*) $\frac{1}{2}\mathscr{L} < 2l < \mathscr{L}$; (*d*) $2l = \mathscr{L}$; (*e*) $\mathscr{L} < 2l < \mathscr{L}_* < 1\frac{1}{2}\mathscr{L}$; (*f*) $2l = \mathscr{L}_*$; (*g*) $\mathscr{L}_* < 2l < 1\frac{1}{2}\mathscr{L}$; (*h*) $2l = 1\frac{1}{2}\mathscr{L}$; (*i*) $1\frac{1}{2}\mathscr{L} < 2l < 2\mathscr{L}$.

the only difference being that the limiting flow rate q_L is either larger, equal to or smaller than q_E, and has the minimum value $p_0^{\frac{1}{2}}$, whereas for the subcritical case $q_L > q_E$. As in the subcritical case shortening the tube postpones flow limitation, and this is so irrespective of the value of $\mathscr{L}_1(0)$, so that the descending part of the curve for supercritical total pressure in figure 8 applies also for $2l > \mathscr{L}_1(0)$ as long as $2l < \frac{1}{2}\mathscr{L}$. For $2l = \frac{1}{2}\mathscr{L}$, figure 10(*b*) shows that flow limitation takes place at $q_L = p_0^{\frac{1}{2}}$ through the mergence of a collapsed and an inflated solution in the solution $\rho(\xi) \equiv 1$. For $2l > \frac{1}{2}\mathscr{L}$, (figure 10*c*) flow limitation takes place at a value of q_L satisfying $p_0^{\frac{1}{2}} < q_L < q_* < q_E$ through the mergence of two inflated solutions, and it may be seen that lengthening the tube with respect to $\mathscr{L}$ now postpones flow limitation, irrespective of its ratio to $\mathscr{L}_1(0)$, so the ascending part of the curve for supercritical total pressure in figure 8 applies also for $2l > \mathscr{L}_1(0)$ as long as $2l > \frac{1}{2}\mathscr{L}$. The effect of increasing the ratio of the tube length with respect to $\mathscr{L}$ on the bifurcation diagram may also be described as a motion of the curves in figure 10 from a 'nose-down' to a 'nose-up' position. This is also the effect of changing this ratio for $2l > \mathscr{L}_1(0)$. The effect of increasing the ratio of the tube length to $\mathscr{L}_1(0)$ is similar to that for the

subcritical case: more solutions appear at low flow rates, which successively disappear when the flow rate is raised. In order to illustrate the combined effect of these two ratios we may, for example, consider the bifurcation diagrams for $\mathscr{L}_1(0) < 2l < 2\mathscr{L}_1(0)$, as given in figure 11. The diagram for $0 < 2l < \frac{1}{2}\mathscr{L}$ is given in figure 11(*a*), which is almost the same as figure 7(*b*) for subcritical total pressure, the difference being as discussed before when comparing figure 10(*a*) and 7(*a*). In the sequence of figure 11(*a–c*), corresponding to increasing values of $2l/\mathscr{L}$, the motion of the most outward curve from a 'nose-down' to 'nose-up' position may again be noted. For $2l = \mathscr{L}$ the bifurcation diagram is given in figure 11(*d*), and it may be noticed that point A_0, where solutions *ULU*, *ULUL* and *LUL* come together has moved to $q = p_0^{\frac{1}{3}}$, so that at this point the bifurcation is present as found by bifurcation analysis (Reyn & Besjes 1984). Figure 11(*e*) refers to $\mathscr{L} < 2l < \mathscr{L}_* < 1\frac{1}{2}\mathscr{L}$, where $\mathscr{L}_*$ is to be defined below. It differs from the previous figure in that the curve for *ULU* has lost its connection with the curve *ULUL* and makes a connection with the curve *UL* at a point B_0 at $q_0 > p_0^{\frac{2}{3}}$, $\rho_{\min} = 1$, $\rho_{\max} > 1$. Point B_0 represents a solution which extends over one wavelength of a periodic solution with wavelength $\mathscr{L}_2$. It is also the solution into which the solutions *LUL* and *LULU* merge, the latter curve starting where the *ULUL* curve ends: at the point $q = p_0^{\frac{2}{3}}$, $\rho_{\min} = \rho_{\max} = 1$, representing the solution $\rho(\xi) \equiv 1$. The solutions *LULU* indicated by the dotted curve in figure 11(*e*) extend to higher values of q the longer the tube is and may give rise to three solutions *LULU* for $q > p_0$ and $2l$ close to $\mathscr{L}_*$. Here $\mathscr{L}_*$ is the tube length, corresponding to a horizontal inflexion point of the curve *LULU* in figure 9(*d*) for the flow rate q, where such a point on the curve *LULU* appears. The diagram for $2l = \mathscr{L}_*$ is given in figure 11(*f*); the existence of a horizontal inflexion point on *LULU* in figure 9(*d*) is reflected in this figure in that from $q = p_0^{\frac{1}{3}}$ up there are three curves *LULU* which meet at some point for $p_0^{\frac{1}{3}} < q < q_0$, and that one curve for *LULU* continues for higher values of q. Further increase of $2l$ above $\mathscr{L}_*$ detaches the lower *LULU* curve from the other two, which with the *ULUL* curve forms a 'nose-down' curve in figure 11(*g*) and a 'nose-up' curve in figure 11(*i*).

As a final example, in figure 12 a bifurcation diagram is given for $n\mathscr{L}_1(0) < 2l < (n+1)\mathscr{L}_1(0)$, $(n+\frac{1}{2})\mathscr{L} < 2l < (n+1)\mathscr{L}$, which should be considered as the generalization of figure 10(*c*) and 11(*i*). It confirms the general impression that more solutions appear near $q = 0$ if the ratio of tube length to $\mathscr{L}_1(0)$ is raised and that with increasing the flow rate solutions pairwise disappear, in what may be called higher-order flow limitations, until finally two solutions are left which disappear at $q = q_L$, the (first-order) flow-limitation value.

5. Concluding remarks

The main conclusion of this paper is that there may be many solutions to the problem of steady flow through a collapsible tube held open at the ends. This multiplicity arises in two ways. The first is related to the fact that for a wide class of tube laws there are more cylindrical tube shapes into which a given cylindrical elastic tube can be deformed, and which allow a flow of a given total pressure and flow rate. If the tube is held open at the ends, and a pulling force thereby is exerted, corrections to the possible cylindrical shapes will result, but multiplicity will be retained. The second way occurs for positive total pressures and is related to the possibility of area-periodic tube shapes in tubes under longitudinal tension, in particular to the fact that the wavelengths of such shapes are amplitude dependent.

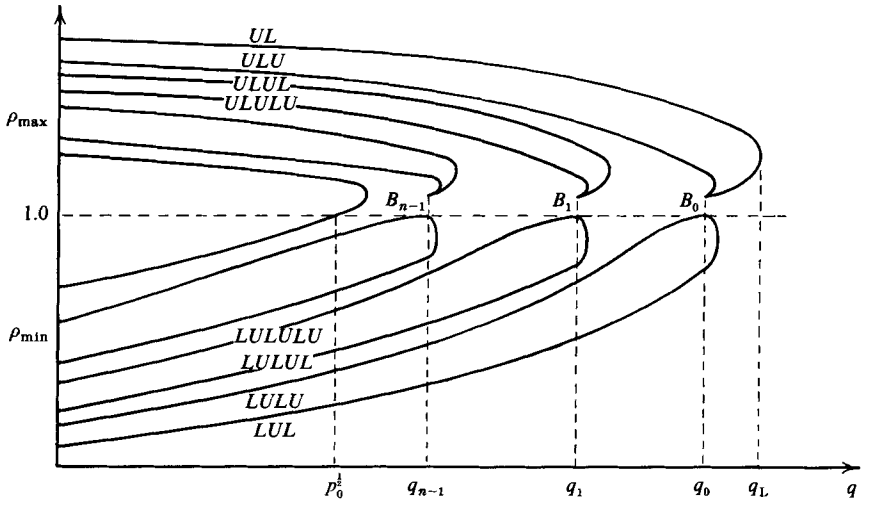

FIGURE 12. Bifurcation diagram for a given tube length and (positive) supercritical total pressures; $n\mathscr{L}_1(0) < 2l < (n+1)\mathscr{L}_1(0)$, $(n+\frac{1}{2})\mathscr{L} < 2l < (n+1)\mathscr{L}$.

Because of these features, the occurrence of a multiplicity of solutions of the boundary-value problem will not critically depend on the particular modelling of the elastic behaviour of the tube wall, and will also remain when this behaviour is described in a more accurate manner.

Other points to be mentioned in relation to the practical implications of the results presented in this paper are stability of solutions and influence of dissipative effects. Although further research would be needed to answer these questions completely, some remarks can already be made on the basis of existing knowledge in the literature. In this respect, the calculations made by Cancelli & Pedley (1985) mentioned in §1 are interesting. For these calculations the collapsible segment, held open by the rigid parts of the circuit, was brought into an initial state where the collapsed segment has uniform area and the velocity is uniform and subcritical. By definition, the total pressure is subcritical, and figure 6(*c*) applies, with the inviscid flow in the uniform tube corresponding to the saddle point. Under these conditions, there also would be another inviscid solution, a collapsed one, involving supercritical flow in the region around the minimum area of the tube, which probably destabilizes the flow. If collapse of the tube is then initiated by increasing the pressure in the surrounding chamber over a short time to a higher constant value, this effectively means, in the present context of measuring pressure differences, that p_0 is decreased at constant flow rate q (some change in τ will also result). As a result, the saddle point in figure 6 shifts to the left, possibly also to the extent that it coincides with the centrepoint and forms a cusp point or that the singular point disappears altogether, and any one of the figure 6(*d–f*) (or figure 3*b–d*) prevails. As long as there is still a singular point there are two solutions for all tube lengths, a subcritical one and one involving also supercritical flow. Apparently, the calculations by Cancelli & Pedley (1985) yielding a stable subcritical solution if the initial-state speed index is low enough and the tension high enough ($u_1 = 0.05$, $\sigma = 4$ in their notation; p. 389), refers to this situation. As in the case with the uniform solution no mention is made of another inviscid solution yielding a more collapsed state of the tube. If the initial speed index is raised and

the tension decreased the collapse process appears to be more drastic, and a region of unsteady supercritical flow appears near the smallest tube area. For the case computed by Cancelli & Pedley (1985) ($u_1 = 0.1$, $\sigma = 2$ in their notation; pp. 388–391) it is not clear whether steady-state solutions are possible. One possibility would be that figure 6(*f*) (or 3*d*) applies, but that the tube is too long to admit steady states. Another possibility is that there are two steady-state solutions, possibly very close to each other, of which, at this moment, is not known whether they contain a supercritical region and what their stability properties are. (Parameter values can be chosen such that this situation occurs with both solutions slightly collapsed and with minor dissipative effects.) Unfortunately, the calculations were stopped at $t = 2058$, when the tube at some point was nearly completely collapsed. That complete collapse is inevitable is not quite clear from a consideration of the immediate approach to steady flow without considerable shift of the narrowest point, and involving the neglect of the longitudinal tension term. In particular if complete collapse occurs, however, and no major changes in the inflow take place, a possibility would be that after $t = 2058$ the constriction continues to move downstream until at the downstream end the tube is opened up again and either an oscillation sets in or a steady state is eventually reached. Even if viscous effects are neglected oscillations of this type could be of practical interest if the collapse time is very small compared with the viscous diffusion time, which in particular would be the case for a downstream rigid part with low resistance and inertia.

In the model developed by Cancelli & Pedley (1985), the magnitude of the friction in regions of attached flow (i.e. upstream of the narrowest point in the tube) is not important; the shape of the tube is not noticeably affected by the inclusion of the friction term. This is a result of the fact that at high values of the Reynolds number, viscous friction and energy dissipation have a relatively small effect when the flow is attached, unless the cross-sectional area becomes very small, and a large effect when flow separation occurs. The pressure recovery in the diverging region of the tube when flow separation occurs was taken into account through use of a constant χ in the momentum equation, where $\chi = 1$ if there is no energy loss (no separation), and $\chi = 0$ if there is no pressure recovery, and in the calculations by Cancelli & Pedley (1985) the values $\chi = 0.2$ and 0.5 were used. In the same way the calculations in this paper may be adjusted to separated flows, simply through replacing q^2 by χq^2 in (3), (7) and (24). Separation would set in for a certain adverse pressure gradient, which in the phase plane leads to the condition that there is separation for $\mathrm{d}\rho/\mathrm{d}\xi > \frac{1}{4}\gamma_1\rho$ and reattachment again for $\mathrm{d}\rho/\mathrm{d}\xi < \frac{1}{4}\gamma_2\rho$, where $\gamma_2 < \gamma_1$ since there is hysteresis in the separation process. (In the paper by Cancelli & Pedley the values 0.2 and 0.3 were selected for γ_1 and 0.05 and 0.1 for γ_2.) Steady-state solutions with separation, as depicted in figure 9 of Cancelli & Pedley (1985), could be reproduced by integration of (24) and traced in the phase plane. In figure 6(*d*) then, the curve LU to the right of the saddle point would be followed starting at the point L and continuing till the line $\mathrm{d}\rho/\mathrm{d}\xi = \frac{1}{4}\gamma_1\rho$ is reached. Then, by making a value of χ not equal to 1, a change of the phase portrait takes place, resulting in a shift of the saddle point to the left and of the centrepoint to the right. A continuation along the integral curve towards the point U yields the shape of the tube in the separated region. In this way, a quantitative basis for comparison with experimental results is obtained, which may be used as a quantitative check on the assumptions made in the present model.

Solutions with area waves are associated with supercritical flow and have been observed experimentally by Kececioglu *et al.* (1981), who studied steady, supercritical flow in collapsible tubes under longitudinal tension. The tube was held open at its

downstream end at its original diameter and compressed by an adjustable sphincter nozzle at the upstream end. For sufficiently high downstream pressures shock-like transitions to subcritical inflated states, with positive transmural pressure, occur and a train of standing area waves appears upstream of the 'shock'. The boundary-value problem associated with this situation is different from that discussed in this paper and it is clear from the start that dissipative effects play a large role, because of the separation that undoubtedly will occur in the 'shock'. If the tube shape is traced in the phase plane, a curve would be found that starts in some point inside the separatrix loop of a phase portrait corresponding to inflow values of p_0, q and τ, and which spirals out, around the centrepoint, with p_0 and τ shifting to end at some point on the ρ-axis, where the flow is subcritical. The spiralling of the curve corresponds to the observed streamwise growth of the standing waves, and unlike the subcritical flow discussed before, the skin friction, and in particular its oscillatory component, is given as an explanation of this growth by McClurken *et al.* (1981). If dissipative effects are taken into account through the effects of separation, while neglecting skin friction, and this is done by replacing q^2 by χq^2 $(0 < \chi < 1)$ if $\mathrm{d}\rho/\mathrm{d}\xi > \frac{1}{4}\gamma_1\rho$ (and once started separation remains as long as $\mathrm{d}\rho/\mathrm{d}\xi > \frac{1}{4}\gamma_2\rho$, where $\gamma_2 < \gamma_1$), a spiralling-out integral curve may also be obtained. This may be demonstrated as follows. For simplicity assume that $\gamma_1 = \gamma_2 = 0$ and p_0 is constant, then in the lower half-plane there exist halves of closed curves nested around a centrepoint for q^2, which is to the left of the centrepoint for $\chi q^2 (\chi < 1)$ around which halves of closed curves in the upper half-plane are clustered. If these curves are traversed in a clockwise direction a spiral curve emerges.

REFERENCES

Bertram, C. D. 1982 Two modes of instability in a thick-walled collapsible tube conveying a flow. *J. Biomech.* **15**, 223–224.

Bertram, C. D. & Pedley, T. J. 1982 A mathematical model of unsteady collapsible tube behaviour. *J. Biomech.* **15**, 39–50.

Bonis, M. & Ribreau, C. 1978 Étude de quelques propriétés de l'écoulement dans une conduite collabable. *Houille Blanche* **3**, 165–173.

Brower, R. W. & Scholten, C. 1975 Experimental evidence on the mechanism for the instability of flow in collapsible vessels. *Med. Biol. Engng* **13**, 839–845.

Cancelli, C. & Pedley, T. J. 1985 A separated-flow model for collapsible-tube oscillations. *J. Fluid Mech.* **157**, 375–404.

Conrad, W. A. 1969 Pressure-flow relationships in collapsible tubes. *IEEE Trans. Bio-med. Engng BME*-16, 284–295.

Griffiths, D. J. 1977 Oscillations in the outflow from a collapsible tube. *Med. Biol. Engng. Comput.* **15**, 357–362.

Hartog, J. P. den 1952 *Advanced Strength of Materials*, p. 73. McGraw Hill.

Katz, A. I., Chen, Y. & Moreno, A. H. 1969 Flow through a collapsible tube. *Biophys. J.* **9**, 1261–1279.

Kececioglu, I., McClurken, M. E., Kamm, R. D. & Shapiro, A. H. 1981 Steady, supercritical flow in collapsible tubes. Part 1. Experimental observations. *J. Fluid Mech.* **109**, 367–389.

Lyon, C. K., Scott, J. B., Anderson, D. K. & Wang, C. Y. 1981 Flow through collapsible tubes at high Reynolds numbers. *Circulation Res.* **49**, 988–996.

McClurken, M. E., Kececioglu, I., Kamm, R. D. & Shapiro, A. H. 1981 Steady, supercritical flow in collapsible tubes. Part 2. Theoretical studies. *J. Fluid Mech.* **109**, 391–415.

Pedley, T. J. 1980 *The Fluids Mechanics of Large Blood Vessels*, chap. 6. Cambridge University Press.

Reyn, J. W. 1982 Equations for the flow of an incompressible, inviscid flow through a collapsible tube under longitudinal tension. *Reports of the Department of Mathematics and Informatics, no.* 82–19. Delft University of Technology, Delft, 27 pp.

REYN, J. W. & BAKKER, P. G. 1984 Steady incompressible inviscid flow through a finite collapsible tube under longitudinal tension. *Reports of the Department of Mathematics and Informatics, no.* 84–01. Delft University of Technology, Delft, 39 pp.

REYN, J. W. & BESJES, J. G. 1984 Flow through finite collapsible tubes: a branching problem. *Reports of the Department of Mathematics and Informatics, no.* 84–29. Delft, University of Technology, Delft, 32 pp.

SCHOENDORFER, D. W. & SHAPIRO, A. H. 1977 The collapsible tube as a prosthetic vocal source. *Proc. San Diego Biomed. Symp.* **16**, 349–356.

SHAPIRO, A. H. 1977 Steady flow in collapsible tubes. *Trans. ASME* K: *J. Biomech. Engng* **99**, 126–147.

UR, A. & GORDON, M. 1970 Origin of Korotkoff sounds. *Am. J. Physiol.* **218**, 524–529.